JOURNAL OF GUIDANCE, CONTROL, AND DYNAMICS
Vol. 35, No. 2, March–April 2012

Engineering Notes

Design and Maintenance of Low-Earth Repeat-Groundtrack Successive-Coverage Orbits

Xiaofeng Fu,* Meiping Wu,† and Yi Tang‡
National University of Defense Technology, Changsha, 410073, P.R.China

DOI: 10.2514/1.54780

I. Introduction

REPEAT-GROUNDTRACK orbits allow a satellite to reobserve any particular spot within the predefined period of time and have been employed in a number of Earth-observation and Earth-science missions, such as LANDSAT, SPOT, ENVISAT, RADARSAT and JASON [1]. Such orbits have, of course, clear military and intelligence applications as well.

In the design and maintenance of a repeat-groundtrack orbit, effects from a nonspherical Earth and atmospheric drag need to be taken into account, as these factors are the primary causes of the groundtrack drift of low-Earth orbits. In missions that require precise groundtracks, the second term of the zonal geopotential harmonics has proven to be insufficient [1]. With such stringent requirements, higher orders of the geopotential harmonics have to be included in the orbit analysis and control. This was done by Vincent [2], and further investigation regarding orbit evolution caused by tesseral harmonics was presented by Ely and Howell [3]. Their work is useful when considering orbit propagation and has been employed in subsequent studies involving orbit design and maintenance. An example using repeat-groundtrack orbits is found in the work of Aorpimai and Palmer [1], in which a geopotential with an arbitrary number of terms in the spherical harmonics was included. The design and maintenance of a low eccentricity orbit for target access, based on the Gaussian equations, was considered by Sengupta et al. [4]. In all these studies, the groundtrack drift at equator crossing (GDEC) is used to evaluate the performance of the orbit maintenance strategy. However, GDEC does not describe the extent of drift at middle and high latitudes. Consequently, orbit maintenance strategies based on GDEC cannot ensure a high level of accuracy over the entire groundtrack, which may be crucial in some missions, such as JASON [5] and ENVISAT [6].

Responsive orbits are those intended to meet the needs of responsive missions. They have the potential to provide means for communications and high-resolution surveillance anywhere in the world within hours of an identified demand [7]. In visual or radar observation missions, responsive orbits can be used to rapidly acquire information of given ground targets and are always low-altitude and circular to achieve responsiveness and high ground resolution. A low-Earth successive-coverage orbit, a subtype of responsive orbits, can provide coverage of a given ground target for several successive orbits every day [7,8] and is suitable for Earth-observation and Earth-science missions. If a low-Earth successive-coverage orbit could repeat its groundtrack, it would allow for specific observations to be scheduled under exactly the same sensing conditions on a routine basis [9].

In this paper, a strategy for design and maintenance of a low-Earth repeat-groundtrack successive-coverage orbits will be presented to achieve high-precision groundtracks. This orbit maintenance strategy is explained based on an analysis of drift over the entire groundtrack (not just GDEC); It not only can keep the GDEC below a given threshold, but it also ensures the accuracy of the entire groundtrack.

II. Groundtrack Drift

The most important perturbations encountered by a low-Earth orbit are caused by the nonspherical nature of the Earth and atmospheric drag. Sectoral and tesseral geopotential harmonics have no secular effect on the semimajor axis, a, eccentricity, e, and inclination, i, of orbits. For a circular orbit, the only secular change that results in groundtrack drift arises in the right ascension of the ascending node (RAAN), Ω. The secular change of the RAAN is given by

$$\frac{\mathrm{d}\Omega}{\mathrm{d}t} = \frac{r \sin u}{na^2\sqrt{1-e^2}\sin i} g_h \tag{1}$$

where r denotes the current radius of the orbit, u denotes the argument of latitude, n denotes the mean motion, and g_h denotes the external acceleration in the out-of-plane direction [4]. Equation (1) allows a geopotential with an arbitrary number of terms in the spherical harmonics to be included until satisfactory accuracy has been achieved [1,4].

Atmospheric drag causes a slow decay in the orbit, reducing altitude as well as eccentricity [4]. This causes an eastward drift of the groundtrack due to a reduced orbital period [1].

The derivative of the semimajor axis of a low-Earth circular orbit caused by atmospheric drag is given by

$$\frac{\mathrm{d}a}{\mathrm{d}u} = -\frac{C_D A}{m} a^2 \rho \tag{2}$$

or

$$\frac{\mathrm{d}a}{\mathrm{d}t} = -\frac{C_D A}{m} na^2 \rho \tag{3}$$

where C_D denotes the atmospheric drag coefficient, A denotes the satellite cross-sectional area, m denotes the satellite mass, and ρ denotes the atmospheric density[10,11].

The orbital period, T, is given by

$$T = T_0 + \int_{u_0}^{u} \frac{\mathrm{d}T}{\mathrm{d}u}\,\mathrm{d}u \tag{4}$$

where T_0 denotes the orbital period at time t_0, and u_0 denotes the argument of latitude at that point. The derivative of orbital period with respect to the argument of latitude, $\mathrm{d}T/\mathrm{d}u$, is given by

$$\frac{\mathrm{d}T}{\mathrm{d}u} = 3\pi\sqrt{\frac{a}{\mu}}\frac{\mathrm{d}a}{\mathrm{d}u} \tag{5}$$

where μ is the gravitational parameter of the Earth.

Received 9 May 2011; revision received 1 September 2011; accepted for publication 4 September 2011.

*Ph.D. Candidate, College of Mechatronics Engineering and Automation; nordicnavigation@hotmail.com (Corresponding Author).

†Research Professor, College of Mechatronics Engineering and Automation; meipingwu@263.net.

‡Ph.D. Candidate, College of Mechatronics Engineering and Automation; tongygood@sohu.com.

The perturbations would cause radial offsets in the orbit as well as changes in the circumferential and out-of-plane directions. Radial and circumferential offsets can be neglected when projected onto the groundtrack (the projection of a radial offset is zero, and the projection of a circumferential offset can be compensated by orbital motion). Thus, the out-of-plane orbital offset projected onto the Earth is equal to the groundtrack drift, as shown in Fig. 1. Here, σ_1 denotes the plane of the two-body orbit, i_1 denotes the inclination of the two-body orbit, λ_{N1} denotes the longitude of ascending node (LAN) of the two-body orbit, σ_2 denotes the plane of the actual orbit, i_2 denotes the inclination of the actual orbit, λ_{N2} denotes the LAN of the actual orbit, ϕ is the angle between σ_1 and σ_2, N_1 is the ascending node of σ_1, N_2 is the ascending node of σ_2, C is a node of σ_1 and σ_2, E_σ is the GDEC of the actual orbit, and D_σ is the maximum drift of the groundtrack of the actual orbit.

Using the spherical triangle laws, the following equation is obtained:

$$\cos\phi = -\cos i_1 \cos(\pi - i_2) + \sin i_1 \sin(\pi - i_2)\cos(\lambda_{N2} - \lambda_{N1}) \tag{6}$$

The deviation of inclination, Δi, is

$$\Delta i = i_2 - i_1 \tag{7}$$

the deviation of LAN, $\Delta\lambda_N$, is

$$\Delta\lambda_N = \lambda_{N2} - \lambda_{N1} \tag{8}$$

Using a truncated Taylor series expansion, Eq. (6) can be rewritten as

$$\phi^2 \approx \Delta i^2 + \Delta\lambda_N^2 \sin^2 i_1 \tag{9}$$

As shown in Fig. 1, D_σ is given by

$$D_\sigma = R_e\phi = R_e\sqrt{\Delta i^2 + \Delta\lambda_N^2 \sin^2 i_1} \tag{10}$$

In addition to the nonspherical nature of the Earth and atmospheric drag, D_σ is affected by orbit insertion error and the sun's gravitational attraction. As seen from Eq. (10), D_σ is determined by $\Delta\lambda_N$ and Δi. The first term is caused by the nonspherical nature of the Earth, atmospheric drag, and orbit insertion error. The second term is caused by the sun's gravitational attraction and orbit insertion error [12]. In responsive missions, the time for correcting the insertion error is short (sometimes there is even no time for correction), and Δi may be large enough to make a significant contribution to the groundtrack drifts of satellite orbits. The inclination drift caused by the sun's gravitational attraction is quite small and very slow compared with the contribution to $\Delta\lambda_N$ due to drag, so Δi can be regarded as constant in an analysis of groundtrack drift [12].

E_σ is given by

$$E_\sigma = R_e\Delta\lambda_N \tag{11}$$

E_σ can only describe the groundtrack drift at the equator (the groundtrack drifts at other latitudes may exceed E_σ when $\Delta i > 0$). D_σ, on the other hand, describes the groundtrack drift of the entire orbit. Therefore, the performance of a complete orbit maintenance strategy should be evaluated with D_σ instead of E_σ. If a space mission requires high-precision groundtracks over the entire orbit, only a strategy based on D_σ can fulfill the requirement.

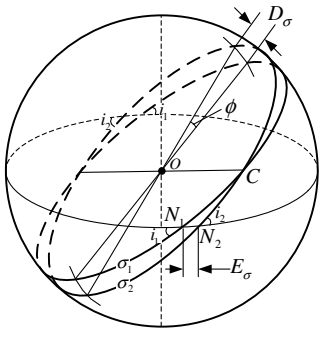

Fig. 1 The maximum drift of the groundtrack and the GDEC.

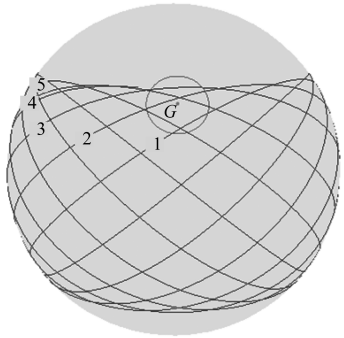

Fig. 2 Ground tracks of a low-Earth successive-coverage orbit.

III. Design of a Low-Earth Repeat-Groundtrack Successive-Coverage Orbit

A satellite in a circular orbit can provide images of the Earth's surface at a constant resolution, and the requirement of periapsis can be neglected if the satellite is launched into a circular orbit. A low-Earth successive-coverage orbit is circular with an inclination 3–5° higher than the latitude of the given ground target [7,8]. This type of orbit not only meets the requirements of constant resolution and responsive launch, but it also provides 3–5 min of coverage of the given ground target per orbit for four or five successive orbits, as shown in Fig. 2 [8,13,14]. In the figure, the numbers 1–5 represent the five successive orbits for coverage, and G denotes the given ground target. Therefore, the eccentricity and inclination are

$$e = 0 \tag{12}$$

$$i = \varphi_G + 5^\circ \tag{13}$$

where φ_G is the latitude of the given ground target.

Suppose that the orbit can repeat its groundtrack once every day. In this case, the following equation is obtained:

$$\frac{2\pi}{T(\omega_e - \dot{\Omega})} = \frac{\sqrt{\mu}}{\sqrt{a^3}(\omega_e - \dot{\Omega})} = k \tag{14}$$

where k is the number of times the satellite orbits the Earth per day, ω_e is the rotation rate of the Earth about its axis, and $\dot{\Omega}$ is the rate of change of the RAAN due to a nonspherical Earth [12]. Here, $k = 15$ or $k = 16$ will hold for low-Earth orbit, and Eqs. (1) and (14) can be solved for the semimajor axis, a. Because k is large, the initial value of the argument of latitude, u_0, makes a negligible contribution to the coverage time and can be safely set to zero [4]:

$$u_0 = 0 \tag{15}$$

Suppose that the launch time is t_{L0} and that the latitude and longitude of the launch site are φ_L and λ_L, respectively. Then, the RAAN of the orbit at the launch time can be given by

$$\Omega = \lambda_L + \bar{S}(t_{L0}) - \arcsin\left(\frac{\tan\varphi_L}{\tan i}\right) \tag{16}$$

where $\bar{S}(t_{L0})$ is the Greenwich mean sidereal time of launch.

IV. Groundtrack Maintenance

The objective of groundtrack maintenance is to keep D_σ below a given drift threshold. D_σ is determined by $\Delta\lambda_N$ and Δi. An orbital inclination adjustment requires out-of-plane impulses, so it is expensive in terms of velocity increment and fuel. Such adjustments should be avoided as long as possible in groundtrack maintenance

[12]. In addition, there is little time for responsive missions to correct the orbital inclination deviation due to insertion error. Thus, in the following discussion, we assume that the groundtrack drifts are controlled by adjusting the semimajor axis.

A. Groundtrack Drift Caused by Drag

Because the effects of a nonspherical Earth have been accounted for in the orbit design, groundtrack maintenance can be performed considering just the perturbation due to atmospheric drag. We take the orbit given by Eqs. (12–16) to be the reference orbit on which the drag is assumed to be zero.

Assuming that the LAN deviation of an actual orbit from the reference orbit due to drag is $\Delta\lambda_D$, the eastward drift of the groundtrack results in that $\Delta\lambda_D$ varies with the increasing latitude argument of the satellite. Suppose the initial value of $\Delta\lambda_D$ is $\Delta\lambda_{D0}$ when the latitude argument of the satellite equals u_0. When the latitude argument of the satellite is u_t, $\Delta\lambda_D$ can be given by

$$\Delta\lambda_D = \int_{u_0}^{u_t} \frac{T_2\omega_e}{2\pi}\,\mathrm{d}u - \frac{T_1\omega_e}{2\pi}(u_t - u_0) + \Delta\lambda_{D0} \tag{17}$$

where T_1 and T_2 are the period of the reference orbit and actual orbit, respectively.

Substituting Eqs. (4) and (5) into Eq. (17) yields

$$\Delta\lambda_D = -\frac{3C_D S\omega_e\rho}{4m}\sqrt{\frac{a_{20}^5}{\mu}}(u_t - u_0)^2 + \frac{\omega_e}{\sqrt{\mu}}(\sqrt{a_{20}^3} - \sqrt{a_{10}^3})(u_t - u_0) + \Delta\lambda_{D0} \tag{18}$$

where a_{10} and a_{20} are the semimajor axes of the reference orbit and actual orbit, respectively, at the initial time t_0 (when the argument of latitude equals u_0). $\Delta\lambda_D$ is a quadratic function of u_t, and its maximum, $\Delta\lambda_{Du}$, is given by

$$\Delta\lambda_{Du} = \frac{m\omega_e(\sqrt{a_{20}^3} - \sqrt{a_{10}^3})^2}{3C_D S\rho\sqrt{\mu a_{20}^5}} + \Delta\lambda_{D0} \tag{19}$$

The derivative of D_σ with respect to u_t is given by

$$\frac{\mathrm{d}D_\sigma}{\mathrm{d}u_t} = \frac{R_e\Delta\lambda_D\sin^2 i}{\sqrt{\Delta i^2 + \Delta\lambda_D^2\sin^2 i}}\frac{\mathrm{d}\Delta\lambda_D}{\mathrm{d}u_t} \tag{20}$$

Thus, D_σ has minima at $\Delta\lambda_D = 0$ and a local maximum at $\mathrm{d}\Delta\lambda_D/\mathrm{d}u_t = 0$, as seen in Fig. 3.

Note that $\Delta\lambda_D$ also has its maximum at $\mathrm{d}\Delta\lambda_D/\mathrm{d}u_t = 0$. The local maximum of D_σ, designated as D_u, can be given by

$$D_u = R_e\sqrt{\Delta i^2 + \Delta\lambda_{Du}^2\sin^2 i} \tag{21}$$

B. Groundtrack Maintenance Strategy

For a circular orbit, a single velocity increment in the orbital plane would cause changes in the semimajor axis and eccentricity:

$$\Delta a = 2a\Delta v_\theta \tag{22}$$

$$\Delta e = \sin f\,\Delta v_r + 2\cos f\,\Delta v_\theta \tag{23}$$

where Δa is the change in the semimajor axis, Δe is the change in the eccentricity, f is the true anomaly, Δv_θ is the velocity impulse in circumferential direction, and Δv_r is the velocity impulse in radial direction [4]. To simplify the attitude control, Δv_θ and Δv_r are usually provided by two different thrusters [15–17], and therefore can be regarded as two distinct impulses.

As seen from Eqs. (22) and (23), the semimajor axis can be altered only with a circumferential velocity impulse; however, this impulse will also change the eccentricity. Therefore, it is impossible to increase the semimajor axis and keep the eccentricity at zero simultaneously with a single velocity impulse; at least two impulses must be used for an orbital transfer.

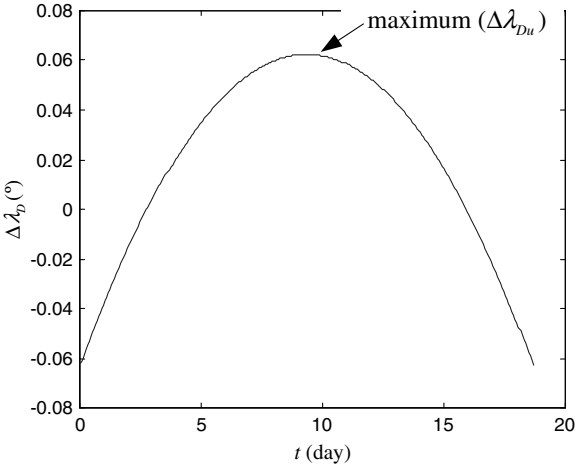

a) Variation of $\Delta\lambda_D$

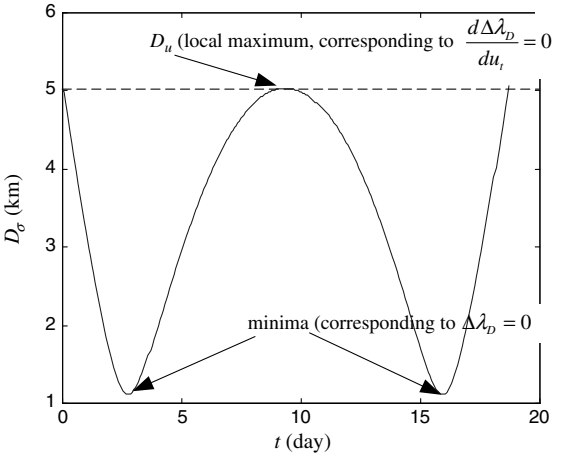

b) Variation of D_σ

Fig. 3 Variations of $\Delta\lambda_D$ and D_σ.

Assuming two impulses are used, the Hohmann transfer is the most fuel-efficient transfer between two circular coplanar orbits [18–21]. The velocity increments are given by

$$\Delta v_{\theta 1} = v_1\left(\sqrt{\frac{2r_2}{r_1 + r_2}} - 1\right) \approx \frac{v_1}{2}\frac{\Delta r}{r_1 + r_2}$$

$$\Delta v_{\theta 2} = v_2\left(1 - \sqrt{\frac{2r_1}{r_1 + r_2}}\right) \approx \frac{v_2}{2}\frac{\Delta r}{r_1 + r_2} \tag{24}$$

where $\Delta v_{\theta 1}$ and $\Delta v_{\theta 2}$ are the velocity increments corresponding to the first and second impulses, respectively, which are both in the circumferential direction. r_1 and v_1 are the radius and velocity of the satellite before the first impulse, r_2 and v_2 are the radius and velocity of the satellite after the second impulse, and Δr is the change in the radial distance of the satellite.

Suppose that the semimajor axis before and after the Hohmann transfer are a_h and a_{20}, respectively. The groundtrack drift must remain below a given threshold, $D_{\lim}$, to ensure the accuracy of the entire groundtrack. The limit on the groundtrack drift yields

$$D_u \le D_{\lim} \tag{25}$$

Then, Eqs. (18), (21), and (25) can be solved for the maximum value of a_{20}, designated as a_{20m}.

The orbit decays slower when the altitude is higher because the atmospheric density decreases with height. If the Hohmann transfer has a larger Δr, the satellite will orbit at a higher altitude and decay

slower, and the time required for groundtrack drift to reach the threshold will be longer. Consequently, the orbit maintenance strategy will be more efficient [12]. Therefore, Δr should reach its maximum value, $\Delta r_{\lim}$, in every orbital transfer to maximize the efficiency of maintenance [12], where

$$\Delta r_{\lim} = a_{20m} - a_h \tag{26}$$

Substituting $D_\sigma = D_{\lim}$ into Eqs. (10) and (18), the maximum latitude argument of a satellite orbiting freely after the orbital transfer, $u_{D\lim}$, can be obtained, and the corresponding flight time, $t_{D\lim}$, can be derived from

$$u_t - u_0 = \int_{t_0}^{t} n\,\mathrm{d}t = \int_{t_0}^{t} \sqrt{\frac{\mu}{(a_{20m} + \dot{a}t)^3}}\,\mathrm{d}t \tag{27}$$

where $\dot{a}$ is the $\mathrm{d}a/\mathrm{d}t$ in Eq. (3). To ensure the groundtrack drift does not exceed the given threshold, orbit maintenance should be performed at or before $t_{D\lim}$.

Because the maintenance occurs on or before the groundtrack drift reaches the given threshold, the satellite would perform maintenance multiple times in a long duration. Therefore, the maintenance efficiency, J, can be evaluated by the mean velocity increment per second:

$$J = \frac{\Delta v_{\theta 1} + \Delta v_{\theta 2}}{t_D + 0.5T} \tag{28}$$

where t_D is the interval between neighboring maintenances, which is called the maintenance interval [4].

The orbit maintenance strategy based on D_σ has been exhibited. In addition, some missions do not need a precise inclination, in which case the inclination deviation can be neglected. Substituting $\Delta i = 0$ into Eq. (10) yields

$$D_\sigma = R_e \Delta\lambda_N \sin i = E_\sigma \sin i \tag{29}$$

Here D_σ is proportional to E_σ, for the atmospheric drag has no effect on the inclination. Equation (21) can be rewritten as

$$D_u = \frac{m\omega_e \sin i R_e(\sqrt{a_{20}^3} - \sqrt{a_{10}^3})^2}{3C_D S\rho\sqrt{\mu a_{20}^5}} + R_e \sin i \Delta\lambda_{D0} \tag{30}$$

If the threshold for GDEC is $E_{\lim}$, then an orbit maintenance strategy based on E_σ (used in previous studies) will be equivalent to a strategy based on D_σ with the threshold of $E_{\lim}\sin i$. That is to say, the strategy based on E_σ can also ensure the accuracy of groundtracks if Δi can be neglected.

V. Numerical Results

As an illustration, consider a satellite that experiences $k = 15$ orbits per day launched into a low-Earth repeat-groundtrack successive-coverage orbit at latitude of 35.4° and longitude of 103.8° at time 03:23:00UT on 2 June 2010. The elements of the reference orbit at the time when the satellite is passing through the ascending node can be obtained from Eqs. (12–16): $a_{10} = 6864.630$ km, $e = 0$, $i = 45°$, $\Omega = 0°$, and $u_0 = 0°$. It is assumed that the coefficient of drag is $C_D = 2.2$, and the area-to-mass ratio of the satellite is $A/m = 0.02$, m^2/kg. Here, the atmospheric density is approximated by an exponential model [12,22].

Lower altitude makes the orbit decay faster due to the increased effects of atmospheric drag. Therefore, the earlier the orbital transfer is performed, the smaller the velocity impulse needed during the groundtrack maintenance. Figure 4 shows the maintenance efficiency vs maintenance interval in a case. It can be seen from the figure that J increases slowly with t_D. Because a thruster suffers wear during each impulse, the groundtrack maintenance could be performed when D_σ reaches the given threshold [12,23].

The requirements and conditions of groundtrack maintenance are as follows. The orbit is designed to make a reconnaissance satellite fly over a given ground target (or site), such that the distance between the groundtrack and the target (or site) is less than 5 km when the satellite is observing the target (or accessing the site). The inclination deviation is $\Delta i = 0.04°$ [14]. Therefore, the groundtrack drift threshold is $D_{\lim} = 5$ km. The strategy based on D_σ can be simulated using Eqs. (10), (18–21), and (25–27). The groundtrack maintenance could be performed when D_σ equals 5 km. Equations (18), (21), and (25) can be solved for the maximum value of a_{20}, a_{20m}= 6864.861 km, corresponding to the radius change of the satellite during the orbital transfer, $\Delta r_{\lim} = 463$ m (for $a_h = 6864.398$ km). Substituting $D_\sigma = 5$ km into Eqs. (10) and (18), the maximum latitude argument of the satellite orbiting freely after the transfer can be found to be $u_{D\lim} = 1214.3$ rad (i.e., 193 circles plus 146°). Substituting $u_{D\lim}$ into Eq. (27), the corresponding flight time can be obtained: $t_{D\lim} = 12.7$ days.

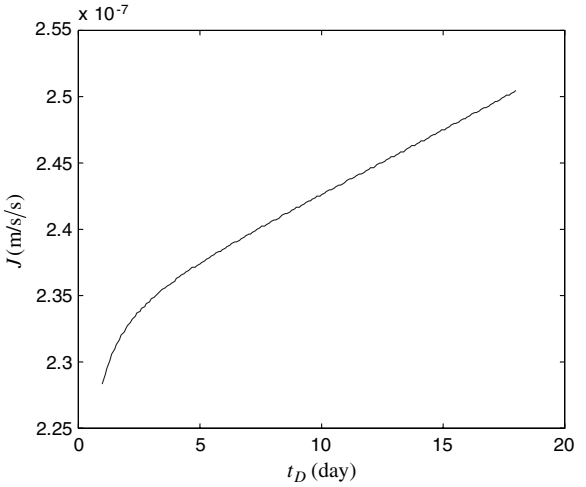

Fig. 4 Maintenance efficiency vs maintenance interval.

In some special circumstances, such as orbit insertion or collision avoidance, the groundtrack deviation of an actual orbit from the reference orbit may exceed the given drift threshold. However, the maintenance strategy based on D_σ will still be able to perform the groundtrack correction. Suppose that the initial groundtrack drift of the actual orbit is 10 km and the inclination deviation is still 0.04°. Substituting the initial groundtrack drift into Eqs. (18), (21), and (25) yields $a_{20m} = 6864.992$ km and $\Delta r_{\lim} = 362$ m (for $a_h = a_{10}$= 6864.630 km). After the groundtrack correction, the satellite resumes the usual orbit maintenance schedule. Figures 5 and 6 exhibit the variations of a and D_σ, respectively. It can be seen from the figures that the groundtrack drift of the actual orbit can be corrected quickly and that the groundtrack drift is always smaller than the threshold $D_{\lim}$.

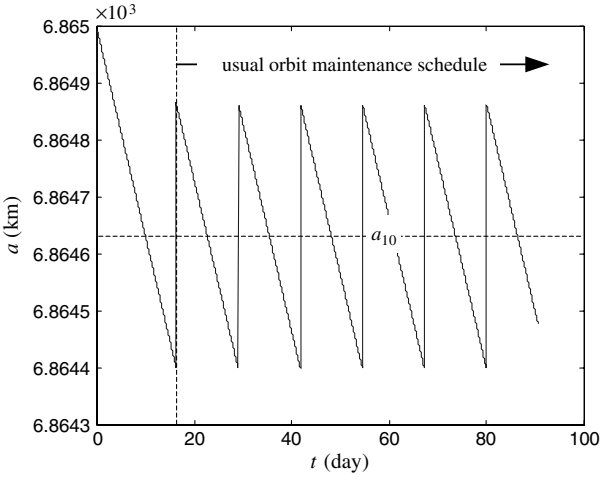

Fig. 5 Variation of the semimajor axis in the strategy based on D_σ.

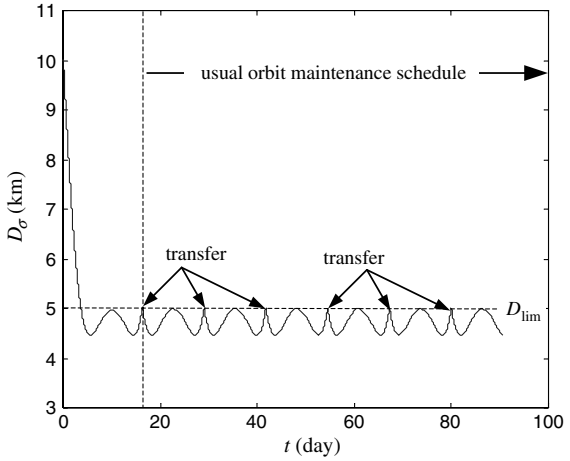

Fig. 6 Groundtrack deviation of an actual orbit from the reference orbit in the strategy based on D_σ.

In the following comparison, we consider an orbit maintenance strategy based on E_σ, as used in previous studies, such as Vallado [12]. For a fair comparison, all other conditions are the same as specified in the preceding paragraph. Note that D_σ and $D_{\lim}$ are not defined in this strategy and that we do not know whether E_σ is larger or smaller than D_σ. In previous studies, the threshold $E_{\lim}$ is provided by the mission requirement to keep equator crossings within an anticipated band. $E_{\lim}$ is regarded as the maximum groundtrack drift [12]; therefore, the threshold should be $E_{\lim} = 5$ km. This strategy can be simulated using Eqs. (11), (18), (27), (28), and (30). Therefore, E_σ would drift between $-E_{\lim}$ and $E_{\lim}$ under control, as shown in Fig. 7. In the figure, the solid line represents D_σ and the dotted line represents E_σ. Obviously, this strategy can keep E_σ below the given threshold, but the actual groundtrack exceeds the anticipated band. The strategy based on E_σ, therefore, cannot achieve the mission requirements (keeping the distance between the groundtrack and the target less than 5 km when the satellite is observing the target).

Because of the inclination deviation, D_σ has a large value all of the time, as shown in Fig. 7. This is also the reason for the failure of the strategy based on E_σ. However, it takes a long time to completely correct an inclination deviation due to orbit insertion error. Therefore, only the strategy based on D_σ can be employed for the maintenance of responsive orbits (including low-Earth repeat-groundtrack successive-coverage orbits), which by definition allow little time to correct the insertion error. The strategy based on D_σ also offers an advantage in any other mission that cannot neglect the inclination deviation, for example missions where the sun's gravitational attraction causes a secular drift of inclination.

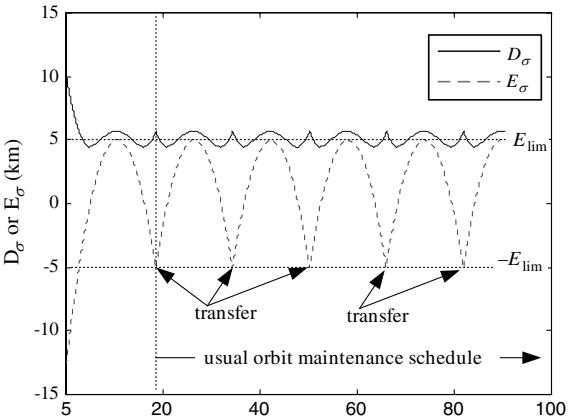

Fig. 7 Groundtrack deviation of an actual orbit from the reference orbit in the strategy based on E_σ.

VI. Conclusion

In this paper, the groundtrack drift caused by the nonspherical nature of the Earth and atmospheric drag was analyzed, and a strategy for the design and maintenance of a low-Earth repeat-groundtrack successive-coverage orbit was presented. In contrast with a traditional analysis of the groundtrack drift at equator crossings over time, this paper discusses the groundtrack drift experienced over the entire orbit in terms of the argument of the latitude. The new strategy evaluates the maximum drift over the entire groundtrack. Therefore, the accuracy of orbit maintenance can be ensured, and the groundtrack drift is kept below a given threshold, not only at the equator, but also along the entire groundtrack. Because this strategy implements orbital transfers based on the groundtrack drift, drift that is caused by factors other than the atmospheric drag can also be corrected.

If the inclination deviation can be neglected, the traditional orbit maintenance strategy (as seen in previous studies) is equivalent to the strategy presented in this paper. That is to say, the traditional strategy can also ensure the accuracy of the entire groundtrack. However, only the presented strategy can fulfill the requirements of high-precision groundtracks in cases where the inclination deviation cannot be neglected, especially regarding responsive missions that allow little time to correct the inclination deviation. Therefore, the maintenance of a low-Earth repeat-groundtrack successive-coverage orbit should be performed using the presented strategy, not the traditional strategy.

The results of this paper are not restricted to low-Earth repeat-groundtrack successive-coverage orbits but are also valid for all other low-Earth orbits.

References

[1] Aorpimai, M., and Palmer, P. L., "Repeat-Groundtrack Orbit Acquisition and Maintenance for Earth-Observation Satellites," *Journal of Guidance, Control, and Dynamics*, Vol. 30, No. 3, 2007, pp. 654–659. doi:10.2514/1.23413

[2] Vincent, M. A., "The Inclusion of Higher Degree and Order Gravity Terms in the Design of a Repeat Ground Track," *AIAA/AAS Astrodynamics Conference*, AIAA Paper 90-2899-CP, Portland, OR, Aug. 1990.

[3] Ely, T. A., and Howell, K. C., "Long-Term Evolution of Artificial Satellite Orbits Due to Resonant Tesseral Harmonics," *Journal of the Astronautical Sciences*, Vol. 44, No. 2, 1996, pp. 167–190.

[4] Sengupta, P., Vadali, S. R., and Alfriend, K. T., "Satellite Orbit Design and Maintenance for Terrestrial Coverage," *Journal of Spacecraft and Rockets*, Vol. 47, No. 1, 2010, pp. 177–187. doi:10.2514/1.44120

[5] Paredes, E., and Navarro, A., "JASON Navigation Shadowing Activities at NASA/JPL for the First Five Years," *AIAA SPACE 2007 Conference & Exposition*, AIAA Paper 2007-6103, Long Beach, CA, Sept. 2007.

[6] Kuijper, D., "Envisat ASAR Interferometry Baseline Results of the Current Envisat Orbit Maintenance Strategy," *SpaceOps 2008 Conference*, AIAA Paper 2008-3205, Heidelberg, Germany, May 2008.

[7] Wertz, J. R., "Coverage, Responsiveness, and Accessibility for Various 'Responsive Orbits'," *3rd Responsive Space Conference*, AIAA Paper RS3-2005-2002, Los Angeles, CA, Apr. 2005.

[8] Wertz, J. R., Van Allen, R. E., and Shelner, C. J., "Aggressive Surveillance as a Key Application Area for Responsive Space," *4th Responsive Space Conference*, AIAA, Paper RS4-2006-1004, Los Angeles, CA, Apr. 2006.

[9] Vtipil, S. D., and Newman, B., "Determining an Efficient Repeat Ground Track Method for Earth Observation Satellites: For Use in Optimization Algorithms," *AIAA, AIAA/AAS Astrodynamics Specialist Conference*, AIAA Paper 2010-8266, Toronto, ON, Canada, Aug. 2010.

[10] Wertz, J. R., and Larson, W. J., *Space Mission Analysis and Design*, 3rd ed., Microcosm Press and Kluwer Academic Publishers, El Segundo, CA and Dordrecht, The Netherlands, 1999, pp. 146–153, 741–742.

[11] Mishne. D., "Formation Control of Satellites Subject to Drag Variations and J2 Perturbations," *Journal of Guidance, Control, and Dynamics*, Vol. 27, No. 4, 2004, pp. 685–692. doi: 10.2514/1.11156

[12] Vallado, D. A., *Fundamentals of Astrodynamics and Applications*, Microcosm Press, Hawthorne, CA, 2007, pp. 858–869.
[13] Wertz, J. R., "ORS Mission Utility and Measures of Effectiveness," *3rd Responsive Space Conference*, AIAA Paper RS6-2008-1003, Los Angeles, CA, Apr. 2008.
[14] Wertz, J. R., *Responsive Space Mission Analysis and Design*, Microcosm, Inc. short course notes, Hawthorne, CA, 2008.
[15] Anzel, B. M., "Method and Apparatus for a Satellite Station Keeping," U.S. Patent 5443231, filed 22 Aug. 1995.
[16] Losa, D., Lovera, M., Marmorat, J. P., Dargent, T., and Amalric, J., "Station Keeping of Geostationary Satellites with On-Off Electric Thrusters," *Proceeding of the 2006 IEEE International Conference on Control Applications*, IEEE, Munich, Germany, Oct. 2006.
[17] Murphy, G. A., "CASTOR: Cathode/Anode Satellite Thruster for Orbital Repositioning," KSC, Rept. KSC-2010-165., April 2010.
[18] Pontani, M., "Simple Method to Determine Globally Optimal Orbital Transfers," *Journal of Spacecraft and Rockets*, Vol. 32, No. 3, 2009, pp. 899–914. doi:10.2514/1.38143
[19] Prussing, J. E., "Simple Proof the Global Optimality of the Hohmann Transfer," *Journal of Guidance, Control, and Dynamics*, Vol. 15, No. 4, 1992, pp. 1037–1038.
doi:10.2514/3.20941
[20] Yuan, F., and Matsushima, K., "Strong Hohmann Transfer Theorem," *Journal of Guidance, Control, and Dynamics*, Vol. 18, No. 2, 1995, pp. 371–373.
doi:10.2514/3.21394
[21] Hazelrigg, G. A., "Globally Optimal Impulsive Transfers via Green's Theorem," *Journal of Guidance, Control, and Dynamics*, Vol. 7, No. 4, 1984, pp. 462–470.
doi:10.2514/3.19879
[22] Humi, M., "Low-Eccentricity Elliptic Orbits in a Central Force Field with Drag," *Journal of Guidance, Control, and Dynamics*, Vol. 33, No. 5, 2010, pp. 1368–1375.
doi:10.2514/1.48693
[23] Shapiro, B., and Pino, A., "Maintenance of an Exact Repeat Ground Track—The GEOSAT ERM," *AIAA, AIAA/AAS Astrodynamics Specialist Conference*, AIAA Paper 1988-4301, Minneapolis, MN, Aug. 1988.